

**HHS PUBLIC ACCESS**

Author manuscript

Nanoscale. Author manuscript; available in PMC 2016 May 11.

Published in final edited form as:

Nanoscale. 2016 March 31; 8(14): 7371–7376. doi:10.1039/c5nr07806g.**Stem cell secretome-rich nanoclay hydrogel: a dual action therapy for cardiovascular regeneration†****Renae Waters^a, Settimio Pacelli^a, Ryan Maloney^a, Indrani Medhi^b, Rafeeq P. H. Ahmed^c, and Arghya Paul^a**Arghya Paul: arghyapaul@ku.edu^aBioIntel Research Laboratory, Department of Chemical and Petroleum Engineering, Bioengineering Graduate Program, School of Engineering, University of Kansas, Lawrence, KS, USA^bSRM University, Kattankulathur 603203, Tamilnadu, India^cDepartment of Pathology, University of Cincinnati, 231-Albert Sabin Way, Cincinnati 45267, OH, USA**Abstract**

A nanocomposite hydrogel with photocrosslinkable micro-porous networks and a nanoclay component was successfully prepared to control the release of growth factor-rich stem cell secretome. The proven pro-angiogenic and cardioprotective potential of this new bioactive system provides a valuable therapeutic platform for cardiac tissue repair and regeneration.

Nanocomposite hydrogels have emerged as a valuable tool in tissue engineering and regenerative medicine as they provide tunable platforms to facilitate the formation of functional tissues.^{1–3} In addition, they can be used as a carrier of drugs or growth factors by selecting a suitable nanomaterial, which can efficiently interact with the loaded biomolecule.⁴ Specifically, the surface area, charge density and presence of reactive functionalities of the nanomaterial are the major parameters that dictate the loading efficiency and release kinetics. A variety of nanoscale materials are available for these applications, such as synthetic polymers, carbon-based nanotubes (CNTs), graphene oxide (GO) and nanodiamonds.^{5–8}

These nanomaterials have been successfully embedded in polymeric networks as a delivery platform for therapeutics. However, their clinical potential in regenerative medicine, particularly for carbon based materials, is currently limited by inefficient loading of multiple therapeutic molecules, non-ideal release kinetics, biodegradability and associated cytotoxicity.^{9,10}

A possible alternative to address these problems is the use of biodegradable, biocompatible, two dimensional synthetic nanoclay materials.¹¹ LAPONITE® ($\text{Na}^{0.7+} [(\text{Si}_8\text{Mg}_{5.5}\text{Li}_{0.3})$

†Electronic supplementary information (ESI) available. See DOI: 10.1039/c5nr07806g

Correspondence to: Arghya Paul, arghyapaul@ku.edu.

$\text{O}_{20}(\text{OH})_4]^{0.7-}$) is an example of synthetic clay from the smectite family that consists of disk-shaped particles with a diameter of approximately 25 nm and a 1 nm thickness.^{12,13} These nanoparticles provide superior physical, chemical, and biological utility when compared to other 2D nanoparticles, such as graphene oxide, due to their uniform shape, discotic charged surface, and high surface-to-volume ratio.¹² These properties allow for anisotropic interactions with anionic, cationic, and neutral polymers to form physically crosslinked networks. In addition, these same interactions can be useful in modulating the release kinetics of drugs and biomolecules.¹⁴ A previous study has reported successful retention and controlled release of vascular endothelial growth factors (VEGF) by adsorbing to the bioactive LAPONITE® surface through electrostatic interactions.¹⁵ The VEGF/LAPONITE® complex was then encapsulated in a collagen scaffold showing enhanced angiogenesis *in vivo* when compared to a collagen scaffold just containing VEGF. This result was attributed to the sustained release in the presence of the synthetic clay.

Nonetheless, scientists have proven that the delivery of multiple growth factors simultaneously can provide an increased therapeutic benefit when compared to monotherapy.^{16–18} This is particularly true for cardiovascular diseases in which a mixture of paracrine growth factors has been shown to promote local angiogenesis and regenerate myocardial tissue. A natural way of producing growth factor-rich conditioned media, also known as secretome, is culturing mesenchymal stem cells (MSCs) under specific stressful conditions such as hypoxia and serum deprivation.

The secretome, isolated from MSCs, has been shown to have cardioprotective abilities, as well as, promote angiogenesis when injected into the *peri*-infarct area.^{19–21} However, the efficacy of this treatment has been hindered by the lack of retention of the secretome components at the site of injury. A nanocomposite hydrogel platform may offer a possible solution to achieve its full therapeutic benefits. This method will also offer an alternate strategy to the widely used stem cell transplantation approach for delivering the paracrine factors.

Here we investigated the possibility of using LAPONITE® nanosilicates and gelatin methacrylate (GelMA) to form a nanocomposite hydrogel for controlled release of stem cell secretome. The overall efficacy of this therapeutic device will be determined following the assessment of two main objectives. First, the effect of nanoclay in controlling the release kinetics of the growth factors present in the secretome needs to be assessed. Second, the pro-angiogenic and cardioprotective ability of the bioactive nanocomposite hydrogel had to be determined. These two aspects are necessary for the successful application of this nanocomposite hydrogel for cardiac regeneration as shown in the schematic (Fig. 1).

To efficiently harness a high concentration of secretome, human bone marrow-derived mesenchymal stem cell (hMSC) spheroids were prepared. This method was chosen because spheroid culture provides a high ratio of cells to media volume that allows for the production of a highly concentrated secretome. Microfabrication technology was used to develop microscale arrayed wells in order to generate the hMSC spheroids.²² Concave microwells (300 μm wide) were fabricated starting from microfluidic channels combined with pentagonal chambers using polydimethylsiloxane (PDMS). Subsequently, a PDMS solution

was introduced into the microfluidic channel filling these chambers. Finally, using suction and a pressing and rolling technique the excess PDMS solution was removed from the chambers. This leads to the production of the concave microwells after curing of the remaining PDMS solution. The formation of this final product is directly attributed to the surface tension of PDMS (Fig. 2A). An hMSC suspension was introduced into the culture device through the inlet port which resulted in a uniform number of cells trapped in each concave well (Fig. 2B). Spheroids were cultured for 48 hours in order to promote the secretion of paracrine factors. The amount of growth factors in the media was quantified using ELISA and compared to hMSCs cultured in 2D under the same conditions. Specifically, the amount of vascular endothelial growth factor (VEGF), fibroblast growth factor 2 (FGF2), angiogenin, and bone morphogenetic protein 2 (BMP2) were found to be significantly higher in the spheroid culture (Fig. 2C). Among all the bioactive molecules, these were chosen due to their integral role in cardiac regeneration by promoting angiogenesis, attenuating apoptotic pathways, and remodelling the damaged myocardium.²³

A possible strategy to improve their therapeutic efficacy is to design a delivery platform that can control their release over time in the site of cardiac injury. For this reason, different nanocomposite photochemical hydrogels based on GelMA and LAPONITE® were fabricated for the delivery of secretome. GelMA is a chemically modified version of gelatin that can easily form a photo-crosslinkable hydrogel due to the presence of methacrylic groups. The systems tested in this study were prepared using GelMA (5.0% w/v) with a medium degree of methacrylation (~50% amine substitution).²⁴ The presence of a microporous network was confirmed by scanning electron microscopy (SEM) (Fig. 2D). The concentration of LAPONITE® was shown to have no effect on the porosity of the hydrogel network (Fig. S1†). The influence of LAPONITE® over the mechanical properties of the photo-crosslinkable hydrogel was investigated through unconfined uniaxial cyclic compression studies (Fig. 2E). As the concentration of LAPONITE® in the GelMA hydrogel was increased from 0.4% to 1% w/v a corresponding enhancement in the mechanical properties was observed. As expected, GelMA hydrogels with the highest concentration of nanoclay showed the greatest Young's Modulus value (Fig. 2F). This observed increase in stiffness is comparable to previously reported results using the same nanocomposite system.¹² These results can potentially be attributed to the electrostatic interactions between the surface of the clay and the polymer chains.²⁵ The very same electrostatic interactions can play a fundamental role in modulating the release of the previously mentioned growth factors. For this reason, the *in vitro* release studies in PBS were carried out for VEGF and FGF2 to assess how the concentration of LAPONITE® could affect their release kinetics (Fig. 2G and H). A better control over the release of VEGF and FGF2 was observed in the formulations containing the higher amount of clay although no significant difference in the swelling behaviour was detected between the groups (Fig. S2†). Specifically, LAPONITE® was able to slow down the amount of growth factors released over time (15 days). This observed effect was directly dependent on clay concentration. We hypothesize that the mechanism responsible for the controlled release of VEGF and FGF2 is mainly due to electrostatic interactions between the growth factors and LAPONITE®, however, hydrogen bonding and ion-dipole interactions could also be involved. In addition, the nanocomposite hydrogels (0.8% and 1.0% w/v), minimized the

initial amount of growth factor detected ($t = 0$). This indicates that the increase in LAPONITE® concentration leads to a more compact matrix capable of better retaining the growth factors for a prolonged period of time. For this reason nanocomposite hydrogels with a concentration less than 0.8% w/v were not further considered in the study.

Next, the angiogenic potential of the hydrogels was tested in order to evaluate the bioactivity of the nanocomposite hydrogel using HUVECs as a model cell line. In particular, nanocomposite hydrogels loaded with secretome were further tested to prove their ability to influence HUVEC proliferation overtime. Growth factors were loaded by mixing the secretome solution with GelMA prior to UV gelation, therefore, it was necessary to verify whether the therapeutic ability of secretome is maintained after the photo-crosslinking process. HUVEC (3×10^6 cells per ml) were encapsulated in three different groups: GelMA hydrogel (Ctrl Gel), GelMA/LAPONITE® hydrogel (NS Gel), and GelMA/LAPONITE® secretome loaded hydrogel (NS Gel+). All of the studies reported used a nanocomposite hydrogel with a LAPONITE® concentration of 0.8% w/v. Results using 1.0% w/v of LAPONITE® were included in the ESI† as the stiffness of the matrix hindered the HUVEC spreading in the 3D polymeric network (Fig. S3†).

At day 3 a statistically significant increase in HUVEC proliferation was observed for the NS Gel+ (Fig. 3A) with respect to the other groups. In addition, the formation of tubular-like structures was more evident in the NS Gel+ system (Fig. 3B) indicating the formation of a more mature cell network. HUVECs were able to spread throughout the total thickness of the NS Gel+ at day 3 (Fig. 3C) as shown by the 3D reconstruction of the gel using confocal imaging. Subsequently, a microchannel migration assay was used to further assess the angiogenesis potential of the NS Gel+ system. The microchannel was fabricated throughout the thickness of the hydrogels by inserting a 200 μm needle into the polymeric solution prior to gelation (Fig. 3D). NS Gel+ showed the greatest potential for lumen formation due to a significant increase in percentage of microchannel area covered ($53.5 \pm 11.7\%$) when compared to the Ctrl Gel ($25.4 \pm 3.3\%$) and NS Gel ($22.6 \pm 6\%$). Overall these findings suggest that the bioactivity of the loaded secretome was not lost after gel formation as demonstrated by the positive influence on HUVEC proliferation and their reorganization into monolayers. These two factors represent fundamental aspects of angiogenesis, which is essential for the regeneration of cardiac tissue.

Apart from angiogenesis, another important mechanism influencing the recovery of cardiac function is the prevention of cell apoptosis and necrosis. Soluble paracrine factors present in secretome have been shown to have an antiapoptotic paracrine effect essential for the improvement of heart function post-infarction.²⁶ For this reason, the antiapoptotic paracrine effect of the secretome loaded nanocomposite hydrogels was another focus of this study.

Cardiomyocytes (CMs) were seeded on the NS Gel+ in 24 wellplate (10^5 cells per well) and cultured for 3 days (Fig. 4A). Fluorescent phalloidin (F-actin) and DAPI (nuclei) staining showed morphology indicative of healthy CMs. (Fig. 4B). Then an induction of cell apoptosis was necessary in order to mimic the conditions present in the post-infarct myocardium. This was accomplished by culturing the cells in hypoxia (1% O_2) and serum deprived conditions (0% FBS) for 24 hours after the confirmation of their beating

functionality. A TUNEL assay was used to detect the presence of apoptotic cells on the different hydrogels characterized by double-stranded DNA breaks (Fig. 4C). In the Ctrl Gel and NS Gel an increase in the presence of red staining was observed, which is indicative of apoptotic cells. On the contrary CMs seeded on the NS Gel+ showed a minimal amount of red staining. This result confirms the cardioprotective ability of secretome which is capable of increasing cardiomyocyte survival and preserving CMs morphology. Specifically, the percentage of apoptotic cells was significantly lower in the NS Gel+ ($15.7 \pm 3.4\%$) than the other groups (Ctrl Gel: $28.6 \pm 1.8\%$; NS Gel: $27.1 \pm 4.9\%$) (Fig. 4D). However, MTS assay showed no significant difference in the amount of necrotic cardiomyocyte cells. Another method to confirm the beneficial anti-apoptotic ability of the loaded secretome in the nanocomposite hydrogels is to quantify the production of reactive oxygen species (ROS). An increase in relative fluorescence intensity, indicative of ROS production, was observed only in the Ctrl Gel and NS Gel, whereas no significant change was detected for the NS Gel+ system after 24 hours of induced apoptosis (Fig. 4E). In addition, activity of Caspase 3/7 was evaluated for 12 hours, as they represent important proteases involved in the execution-phase of cell apoptosis. Throughout the experiment a higher enzymatic activity was detected for the Ctrl Gel and NS Gel compared to the NS Gel+ confirming the protective ability of the loaded secretome in reducing the apoptosis process (Fig. 4F).

Conclusions

In conclusion, we report two principal findings. First, nanoclay can modulate the controlled release of multiple key growth factors present in stem cell derived secretome. The possible mechanism dictating this release profile is electrostatic interactions between the highly charged surface of LAPONITE® nanoplatelets and the growth factors of the secretome. Second, a stem cell derived secretome loaded nanocomposite hydrogel provides a dual action therapeutic system through its proangiogenic and cardioprotective ability. After the hydrogel is implanted into the damaged myocardium, this approach has the potential to increase the therapeutic efficacy of stem cell derived secretome for cardiac regeneration by increasing its retention in the site of injury. Therefore, the encapsulation of stem cell derived secretome in a nanocomposite hydrogel provides a promising alternative to stem cell therapy for the regeneration of cardiac tissue post myocardial infarction.

Methods

Materials

Synthetic silicate nanoplatelets (LAPONITE® XLG) SiO₂ (59.5%), MgO (27.5%), Na₂O (2.8%) and Li₂O (0.8%) with low heavy metals content were supplied by Southern Clay Products, Inc. (Louisville). Gelatin type A from porcine skin, methacrylic anhydride, Irgacure 2959, were used without further modification from the manufacturer (Sigma-Aldrich, St Louis, MO).

Preparation of the nanocomposite hydrogels

Nanocomposite hydrogels were prepared by mixing a GelMA solution (5% w/v) with different concentrations of LAPONITE® (0.4, 0.8, and 1.0% w/v). Irgacure 2959 (0.5%

w/v) was added prior to photoirradiation under UV light. In order to load the nanocomposite hydrogels with secretome 250 μL of polymeric mixture was combined with the 250 μL of media containing secretome prior to photoirradiation. Hydrogels with a thickness of approximately 3.5 mm and a diameter of 4 mm were photocrosslinked at 5 mW cm^{-2} for 10 minutes for mechanical testing. Young's Modulus was calculated using the slope of the stress strain curve in the region up to 10% of strain.²⁷

Harnessing the MSC secretome using a microfluidic device

A microfluidic device was fabricated using a method previously reported.²² hMSCs were first cultured in 2D conditions using DMEM supplemented with 1% L-glutamine, 1% penicillin/streptomycin, and 10% FBS. hMSCs (passage 2–5) were then trypsinized and a 250 μL solution with a cell density of 5×10^6 cells per ml was injected into the device ensuring an even distribution throughout all the wells. The hMSCs were incubated in a vertical position at 37 °C incubator for 48 h to allow formation of spheroids and secretion of paracrine factors in conditioned media (secretome). Quantification of the growth factors in the secretome was carried out using respective ELISA kits (R&D Systems).

Characterization of nanocomposite hydrogels

Compression studies of the nanocomposite hydrogels were investigated using an RSA-III dynamic mechanical analyser (TA Instrument; New Castle, NE). Samples were cyclically compressed ($n = 2$) up to 25% of their original height at a rate of 0.005 mm s^{-1} in order to obtain stress *versus* strain curves. Then, the compressive modulus was calculated as the slope of the stress *versus* strain curve from 0% to 10% strain. After the mechanical characterization, secretome release kinetic studies were carried out. The secretome loaded nanocomposite hydrogels were incubated at 37 °C in 100 μL of phosphate buffer solution (PBS) for 15 days. The PBS was changed every 3 days and ELISA was used to quantify the amount of VEGF and FGF2 in the PBS incubation solution at each time point.

Analysis of angiogenic potential of hydrogels

For cell study purposes, HUVECs were cultured in normal endothelial growth medium with growth supplements (EGM-2 BulletKit without additional VEGF and FGF, Lonza, Walkersville, MD) and 1% penicillin/streptomycin. Passage 6–9 HUVECs were used in all 3D encapsulation experiments. Prior to encapsulation experiments, HUVECs were trypsinized, centrifuged to obtain a pellet, and mixed with GelMA/LAPONITE® polymeric solution under sterile conditions. The HUVEC cell density in the polymer solution was 3×10^6 cells per mL. Each gel was fabricated in a 96 well plate by adding 50 μL of the cell suspended hydrogels from different groups (equal volume of secretome and prepolymer gel for NS+ group). After photocrosslinking for one minute, the gels containing cells were grown for 3 days. Calcein staining was performed to investigate the morphology of the cells and the stained gels were washed with DPBS and high-resolution z-stack images were obtained using a confocal microscope (Olympus FV1200). For the microchannel migration assay, HUVECs were suspended in culture media (without VEGF and FGF) and seeded inside the microchannels. After 36 hours, photomicrographs were taken and analysed in Image J for percentage of area covered by adhered and migrated HUVECs in the different experimental groups.²⁸

Analysis of the cardioprotective properties of hydrogels

All experimental procedures were performed in accordance with the standard human care guidelines of the Guide for the Care and Use of Laboratory Animals published by the US National Institutes of Health (NIH Publication No. 85-23, revised 1996) and protocol No. 15-06-17-01 approved by the Institutional Animal Care and Use Committee, University of Cincinnati. The neonatal CMs used for this study were isolated from newborn (1–3 day) Fisher-344 rat pups using the Worthington Neonatal CMs Isolation System (Worthington Biochemical) following the manufacturer's protocol and earlier published work.²⁹ Minced harvested hearts were enzymatically digested by incubation overnight at 4 °C in trypsin 50 mg mL⁻¹. The tissue was then oxygenated for 1 min and incubated with 5 mL collagenase at a concentration of 300 U mL⁻¹ on the shaker (2–4 rounds per min) for 30–45 min at 37 °C. Following this, the tissue was oxygenated and triturated several times, and undigested tissue was filtered out. The cells were allowed to settle for 20 min at an ambient temperature and centrifuged at 100g for 5 min before preplating twice (45 min each) in DMEM media (Hyclone), supplemented with 10% FBS (Hyclone) and Penicillin/Streptomycin at 37 °C.

After culturing CMs for 48 hours on the hydrogels in 10% FBS and 5% O₂, the culture conditions were changed to 0% FBS and 1% O₂ for 24 hours to induce cell apoptosis. The resulting cell apoptosis was quantified by monitoring Caspase 3/7 activity using an Apo-ONE® Caspase-3/7 Assay (Promega) for 12 hours and using a Dead End™ Colorimetric TUNEL Assay (Promega).^{30,31} Cell necrosis was quantified using an MTS assay. ROS production under previously mentioned stressed condition on different hydrogel formulations was determined by Intracellular ROS assay at 0 hour and 24 hour using fluorescence imaging.

Statistical analysis

Quantitative variables are presented as mean ± Standard Deviation (SD) from independent experiments as described in the figure legends. Statistics were performed using two-way and/or one-way Analysis of variance (ANOVA) by Bonferroni's multiple comparison *post hoc* test. All statistical analyses were performed with Prism 5 (GraphPad Software). *P* value <0.05 was considered significant.

Supplementary Material

Refer to Web version on PubMed Central for supplementary material.

Acknowledgments

R. W. acknowledges the financial support from NIH-Biotechnology Predoctoral Research Training Program (T32-GM008359). A. P. acknowledges the University of Kansas New Faculty General Research Fund for support. The author also acknowledges an investigator grant provided by the Institutional Development Award (IDeA) from the National Institute of General Medical Sciences (NIGMS) of the NIH P20GM103638-04. R. P. A. acknowledges NIH grant No. R01HL106190, R01HL087288 support.

References

1. Haraguchi K. *Curr. Opin. Solid State Mater. Sci.* 2007; 11:47–54.
2. Paul A. *Nanomedicine.* 2015; 10:1371–1374. [PubMed: 25996115]

3. Pacelli S, Manoharan V, Desalvo A, Lomis N, Jodha KS, Prakash S, Paul A. *J Mater. Chem. B*. 2015
4. Song F, Li X, Wang Q, Liao L, Zhang C. *J Biomed. Nanotechnol.* 2015; 11:40–52. [PubMed: 26301299]
5. Li Y, Dong H, Li Y, Shi D. *Int. J. Nanomed.* 2015; 10:2451–2459.
6. Montellano A, Da Ros T, Bianco A, Prato M. *Nanoscale.* 2011; 3:4035–4041. [PubMed: 21897967]
7. Cho H-B, Nguyen S, Nakayama T, Huynh M, Suematsu H, Suzuki T, Jiang W, Rozali S, Tokoi Y, Park Y-H, Niihara K. *J Mater. Sci.* 2013; 48:4151–4162.
8. Paul A, Hasan A, Kindi HA, Gaharwar AK, Rao VT, Nikkhah M, Shin SR, Krafft D, Dokmeci MR, Shum-Tim D, Khademhosseini A. *ACS Nano.* 2014; 8:8050–8062. [PubMed: 24988275]
9. Kostarelos K, Bianco A, Prato M. *Nat. Nanotechnol.* 2009; 4:627–633. [PubMed: 19809452]
10. Krishna KV, Menard-Moyon C, Verma S, Bianco A. *Nanomedicine.* 2013; 8:1669–1688. [PubMed: 24074389]
11. Choy J-H, Choi S-J, Oh J-M, Park T. *Appl. Clay Sci.* 2007; 36:122–132.
12. Gaharwar AK, Mihaila SM, Swami A, Patel A, Sant S, Reis RL, Marques AP, Gomes ME, Khademhosseini A. *Adv. Mater.* 2013; 25:3329–3336. [PubMed: 23670944]
13. Gaharwar AK, Avery RK, Assmann A, Paul A, McKinley GH, Khademhosseini A, Olsen BD. *ACS Nano.* 2014; 8:9833–9842. [PubMed: 25221894]
14. Min J, Braatz RD, Hammond PT. *Biomaterials.* 2014; 35:2507–2517. [PubMed: 24388389]
15. Dawson JI, Kanczler JM, Yang XB, Attard GS, Oreffo RO. *Adv. Mater.* 2011; 23:3304–3308. [PubMed: 21661063]
16. Lu S, Lam J, Trachtenberg JE, Lee EJ, Seyednejad H, van den Beucken JJ, Tabata Y, Wong ME, Jansen JA, Mikos AG. *Biomaterials.* 2014; 35:8829–8839. [PubMed: 25047629]
17. Zhang H, Jia X, Han F, Zhao J, Zhao Y, Fan Y, Yuan X. *Biomaterials.* 2013; 34:2202–2212. [PubMed: 23290468]
18. Ruvinov E, Leor J, Cohen S. *Biomaterials.* 2011; 32:565–578. [PubMed: 20889201]
19. Fidelis-de-Oliveira P, Werneck-de-Castro JP, Pinho-Ribeiro V, Shalom BC, Nascimento-Silva JH, Costa e Souza RH, Cruz IS, Rangel RR, Goldenberg RC, Campos-de-Carvalho AC. *Cell Transplant.* 2012; 21:1011–1021. [PubMed: 22305373]
20. Gallina C, Turinetti V, Giachino C. *Stem Cells Int.* 2015; 2015:765846. [PubMed: 26074978]
21. Stastna M, Van Eyk JE. *Circ.: Cardiovasc. Genet.* 2012; 5:o8–o18. [PubMed: 22337932]
22. Jeong GS, Jun Y, Song JH, Shin SH, Lee S-H. *Lab Chip.* 2012; 12:159–166. [PubMed: 22076418]
23. Gallina C, Turinetti V, Giachino C. *Stem Cells Int.* 2015; 2015:765846. [PubMed: 26074978]
24. Nichol JW, Koshy S, Bae H, Hwang CM, Yamanlar S, Khademhosseini A. *Biomaterials.* 2010; 31:5536–5544. [PubMed: 20417964]
25. Pawar N, Bohidar H. *J Chem. Phys.* 2009; 131:045103–045103. [PubMed: 19655924]
26. Chanyshev B, Shainberg A, Isak A, Chepurko Y, Porat E, Hochhauser E. *Mol. Cell. Biochem.* 2012; 363:167–178. [PubMed: 22160856]
27. Pacelli S, Paolicelli P, Pepi F, Garzoli S, Polini A, Tita B, Vitalone A, Casadei M. *J Polym. Res.* 2014; 21:1–13.
28. Nikkhah M, Eshak N, Zorlutuna P, Annabi N, Castello M, Kim K, Dolatshahi-Pirouz A, Edalat F, Bae H, Yang Y, Khademhosseini A. *Biomaterials.* 2012; 33:9009–9018. [PubMed: 23018132]
29. Konoplyannikov M, Haider KH, Lai VK, Ahmed RP, Jiang S, Ashraf M. *Stem Cells Dev.* 2013; 22:204–215. [PubMed: 22873203]
30. Prabha S, Sharma B, Labhasetwar V. *Cancer Gene Ther.* 2012; 19:530–537. [PubMed: 22595792]
31. Tu Y, Zhu L. *J Controlled Release.* 2015; 212:94–102.

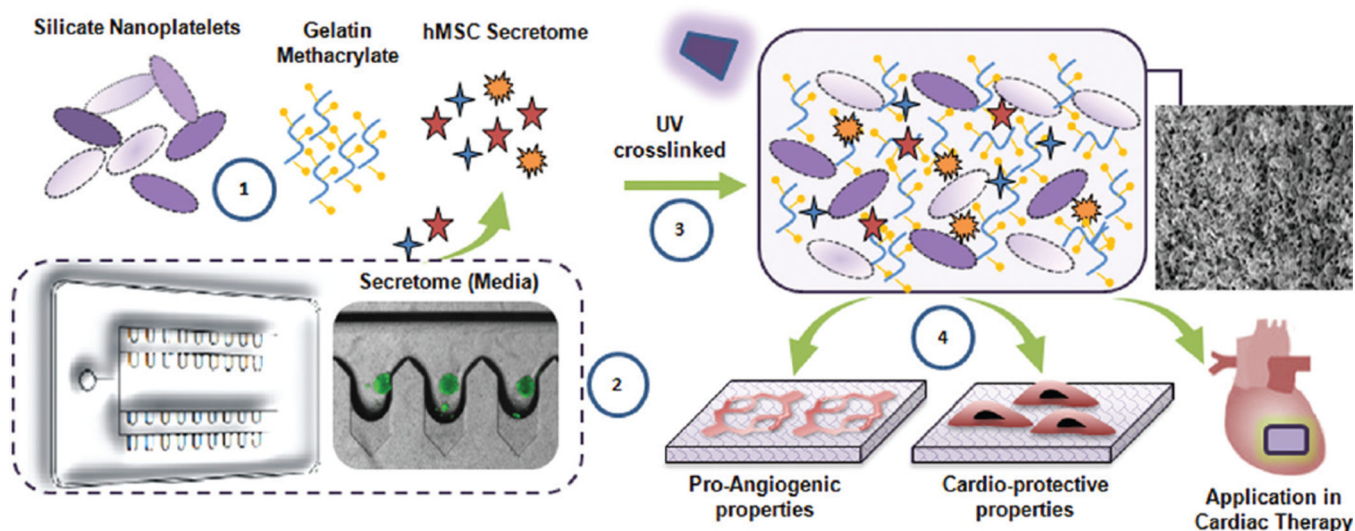


Fig. 1. Concept in schematic. (1) Photo-crosslinkable nanocomposite hydrogels comprised of silicate nanoplatelets, GelMA and hMSC derived growth factors (secretome). (2) Microbioreactor with deep concave wells to harness hMSC secretome. (3) Photo-crosslinked nanocomposite hydrogel encapsulating secretome. (4) The hydrogel can promote endothelial proliferation, migration and significantly attenuate cardiac cell apoptosis under stressed (hypoxic and serum starved) conditions.

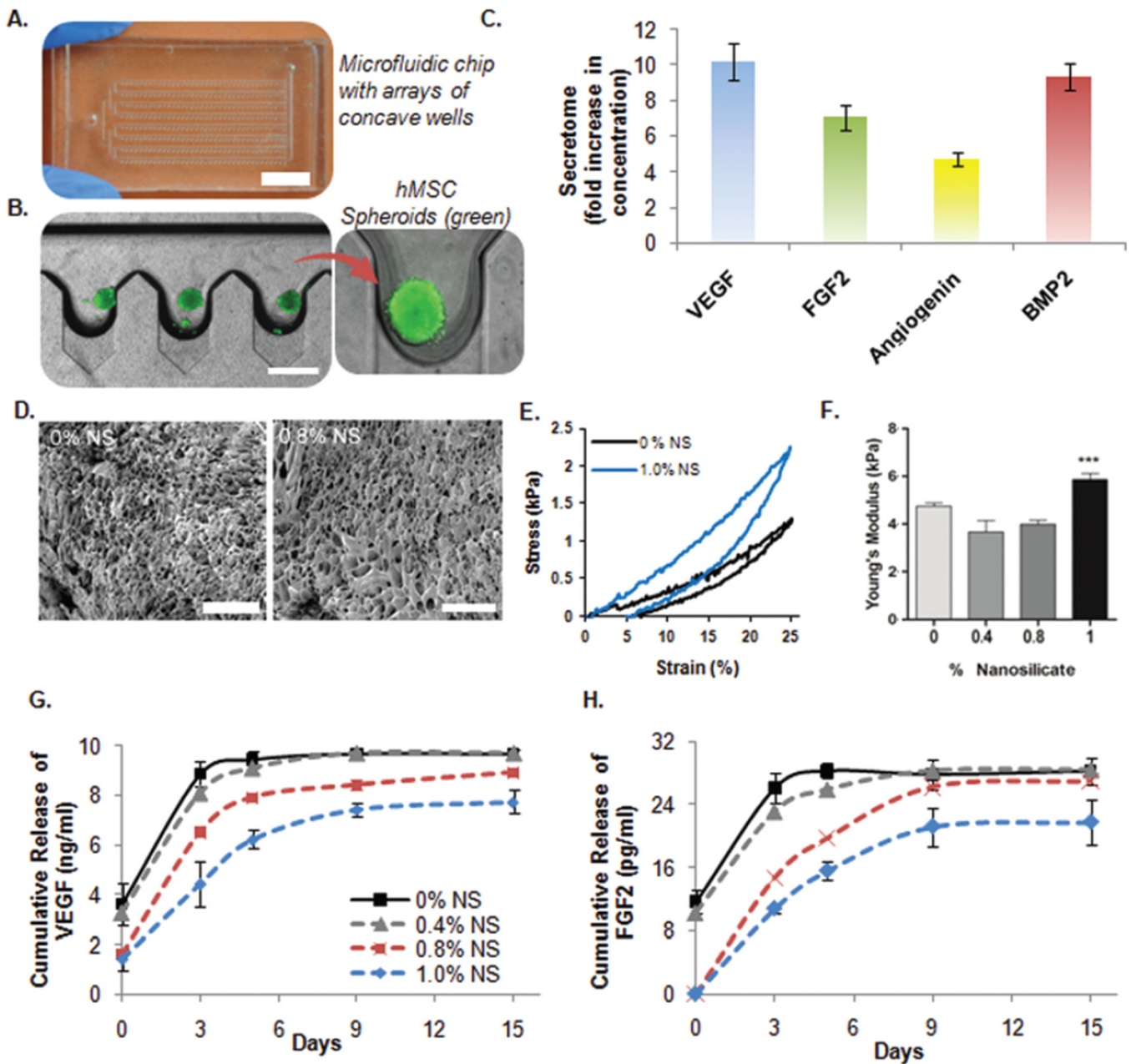


Fig. 2. *In vitro* characterization of the developed nanocomposite hydrogel carrying secretome of hMSC spheroids. (A) Microfluidic chip with concave microwell array. Optical microscopy image of the microfluidic chip (Scale bar: 1 mm). (B) hMSC spheroid formation in the deep concave microwell arrayed microfluidic chip (Scale bar: 500 μ m). (C) After 48 h, the conditioned media (secretome) was harvested from the microfluidic chip leaving behind the spheroids. hMSC spheroids secreted higher concentration of growth factors (VEGF, FGF, Angiogenin and BMP2) compared to 2D culture in plates as quantified by ELISA. (D) Scanning electron microscopic images of 0% and 0.8% NS hydrogels demonstrate the porous microstructures of the hydrogel (Scale bar: 100 μ m). (E and F) Cyclic stress *versus*

strain curves and corresponding compressive modulus of the hydrogel showing the effect of LAPONITE® concentration over the mechanical properties (G and H) Effect of NS concentration on release of VEGF and FGF2 growth factors from different NS hydrogel formulations over time. *** = $P < 0.001$, $n = 3$.

Author Manuscript

Author Manuscript

Author Manuscript

Author Manuscript

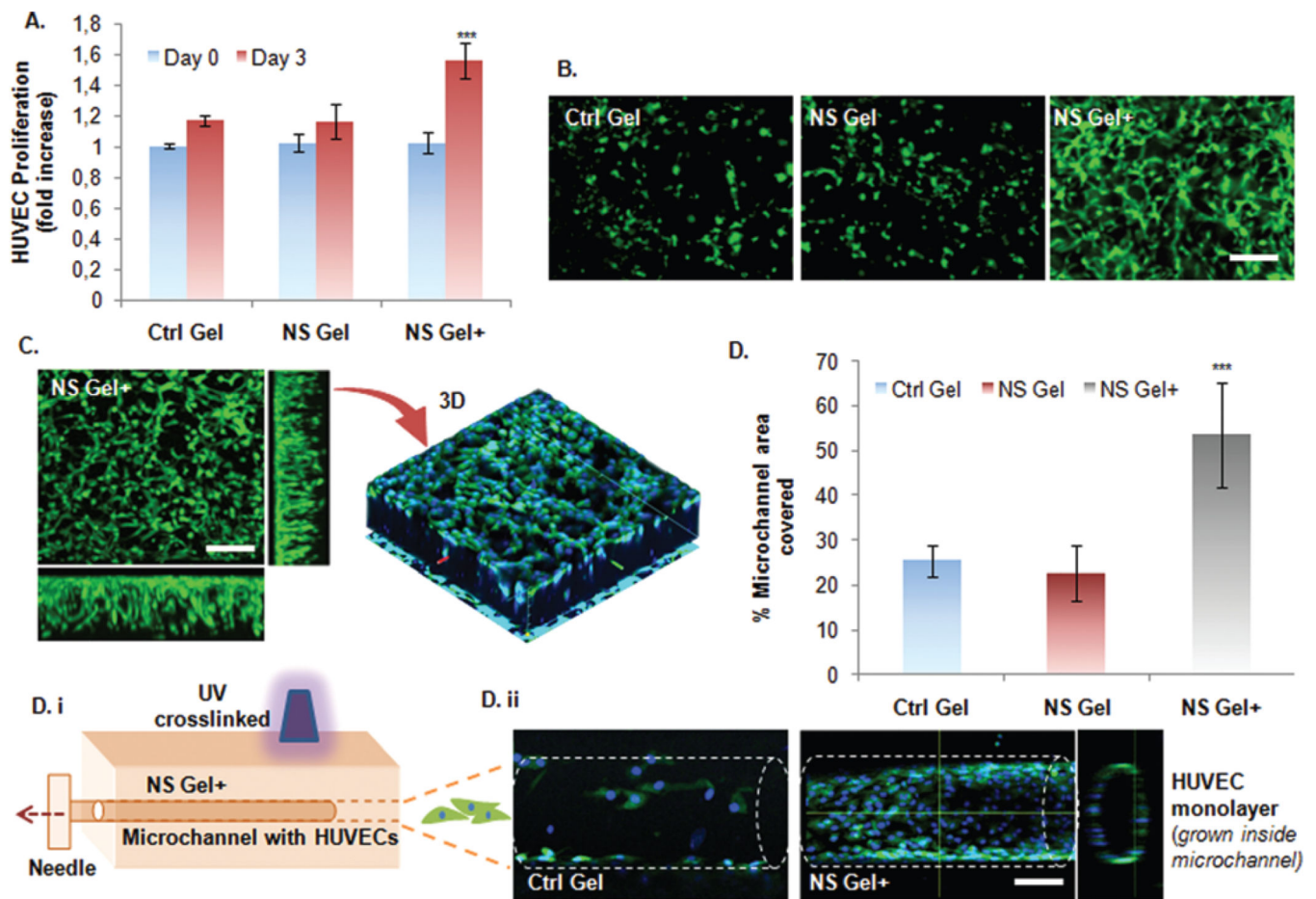


Fig. 3. Angiogenic potential of the developed bioactive nanocomposite hydrogel. (A) Proliferation of HUVECs in 3D hydrogels with (NS Gel+) and without secretome (NS Gel). As a control group, hydrogel without NS (Ctrl Gel) was used. Cell proliferation was detected by MTS colorimetric assay while data ($n = 3$) presented in the graph were normalized with data from the control gel group at Day 0. NS+ Gel group showed significantly higher proliferation compared to other groups. (B) Representative photomicrographs of calcein stained HUVECs encapsulated in each hydrogel group. Importantly, HUVEC in NS+ Gel group also demonstrated highly branched tube-like structures which were absent in other groups. (C) Confocal fluorescence microscope image of HUVECs grown in 3D NS+ hydrogel, with blue nuclei stained with DAPI. The image confirms proliferation of the HUVEC all throughout the thickness of the hydrogel with highly branched tube-like microstructures. (D) i–ii. HUVEC adhesion and migration assay inside microchannels fabricated from the different hydrogel groups. The microchannel was made by needle ($200 \mu\text{m}$) insertions and photocrosslinking. Data are expressed as mean value \pm Standard Deviation (SD). *** = $P < 0.001$ compared to Control Gel, $n = 3$. (Scale bar: $100 \mu\text{m}$).

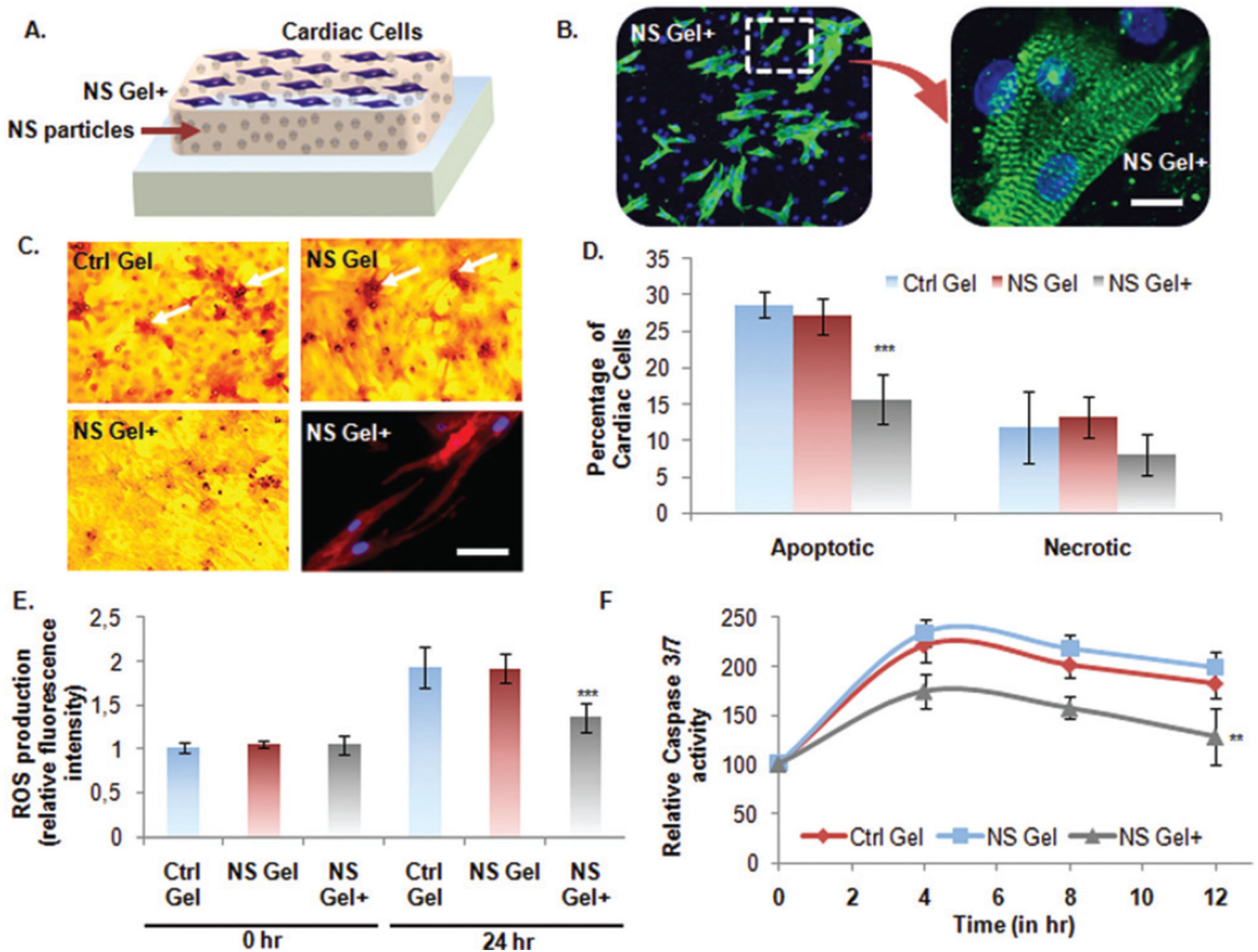


Fig. 4. Cardioprotective nature of the developed bioactive nanocomposite hydrogel. (A) Schematic of culturing neonatal CMs on nanocomposite hydrogels. (B) Fluorescence microscope images of CMs grown in standard condition on NS+ hydrogel. The cells were immunostained with cardiac specific marker, sarcomeric α -actinin, and nuclei with DAPI (Scale bar: 10 μ m). (C and D) Apoptosis assay on CMs under stressed condition by Deadend Colorimetric TUNEL assay. (Scale: bar: 50 μ m). Number of apoptotic cells per well was quantified and represented in graph as percentage apoptotic cells per group. MTS assay was also performed to quantify the percentage of necrotic cells. The picture on lower right panel shows CM cells grown on the NS+ hydrogel under the above mentioned stressed condition still retained expression of intact cardiac marker, sarcomeric α -actinin. (E) Detection of ROS-induced apoptosis. Intracellular ROS quantified in terms of relative fluorescence intensities normalized to Ctrl gel value at 0 h. (F and G) To investigate the anti-apoptotic effects of the NS+ hydrogel, Caspase-3/7 activity was measured as an early indicator of apoptosis using Apo-ONE® homogeneous caspase-3/7 assay Kit (Promega, Madison, WI,

USA). Data are expressed as mean value \pm Standard Deviation (SD). *** = $P < 0.001$ and ** = $P < 0.01$ compared to Control Gel, $n = 3$.

Author Manuscript

Author Manuscript

Author Manuscript

Author Manuscript